RESEARCH ARTICLE

The role of endogenous H_2S formation in reversible remodeling of lung tissue during hibernation in the Syrian hamster

Fatemeh Talaei[1], Hjalmar R. Bouma[1], Machteld N. Hylkema[2], Arjen M. Strijkstra[1,3], Ate S. Boerema[3],
Martina Schmidt[4] and Rob H. Henning[1,*]

[1]Department of Clinical Pharmacology, University of Groningen, University Medical Center Groningen, PO Box 196, 9700 RB Groningen, The Netherlands, [2]Department of Pathology and Medical Biology, University of Groningen, University Medical Center Groningen, 9713 AV Groningen, The Netherlands, [3]Departments of Chronobiology and Molecular Neurobiology, Center for Behavior and Neurosciences, University of Groningen, 9700 RB Groningen, The Netherlands and [4]Department of Molecular Pharmacology, University of Groningen, 9700 RB Groningen, The Netherlands

*Author for correspondence (r.h.henning@umcg.nl)

SUMMARY

During hibernation, small mammals alternate between periods of metabolic suppression and low body temperature ('torpor') and periods of full metabolic recovery with euthermic temperatures ('arousal'). Previously, we demonstrated marked structural remodeling of the lung during torpor, which is rapidly reversed during arousal. We also found that cooling of hamster cells increased endogenous production of H_2S through the enzyme cystathionine-β-synthase (CBS). H_2S suppresses the immune response and increases deposition of collagen. Therefore, we examined inflammatory markers and matrix metalloproteinase (MMP) activity in relation to CBS expression and H_2S levels in lungs of euthermic and hibernating Syrian hamsters. Lung remodeling during torpor was confirmed by a strong increase in both collagenous and non-collagenous hydroxyproline content. The number of leukocytes in lung was unchanged in any phase of hibernation, while adhesion molecules VCAM-1 and ICAM-1, and the inflammatory marker NF-κB (P65) were modestly upregulated in torpor. Gelatinase activity was decreased in lungs from torpid animals, indicating inhibition of the Zn^{2+}-dependent MMP-2 and MMP-9. Moreover, expression of CBS and tissue levels of H_2S were increased in torpor. All changes normalized during arousal. Inhibition of gelatinase activity in torpor is likely caused by quenching of Zn^{2+} by the sulphide ion of H_2S. In accord, inhibition of CBS normalized gelatinase activity in torpid animals. Conversely, NaHS decreased the gelatinase activity of euthermic animals, which was attenuated by excess Zn^{2+}. Similar results were obtained on the activity of the Zn^{2+}-dependent angiotensin converting enzyme. Our data indicate that increased production of H_2S through CBS in hamster lungs during torpor contributes to remodeling by inhibition of gelatinase activity and possibly by suppression of the inflammatory response. Although administration of H_2S is known to induce metabolic suppression in non-hibernating mammals ('suspended animation'), this is the first report implying endogenous H_2S production in natural hibernation.

Key words: *Mesocricetus auratus*, collagen, cystathionine beta synthase, hibernation, hydrogen sulfide, lung remodeling.

INTRODUCTION

Hibernation represents the most radical example of hypometabolism among mammalian species and is characterized by repetitive cycling between well-defined stages. Torpor is the state of metabolic suppression resulting in extreme hypothermia, respiratory depression and low blood pressure in hibernating animals. It is interrupted by bouts of arousal during which metabolism and other parameters normalize (Carey et al., 2003). Notably, the hibernating animal withstands significant organ damage (Arai et al., 2005) and mechanisms applied by hibernators to alleviate organ damage may have potential application to human biology and medicine, addressing issues such as resistance to ischemia and hypothermic organ preservation, prevention of muscle atrophy and even the development of inducible torpor as an aid in acute medicine or surgery (Morin and Storey, 2009; Zancanaro et al., 1999).

Recently, we identified rapid remodeling of the lung during the torpor phase in the Syrian hamster (Talaei et al., 2011b), as shown by the induction of smooth muscle actin mass, increased transforming growth factor-β expression and extracellular matrix

(ECM) collagen deposition by both immunohistochemistry and biochemical analysis. The most striking finding was that these alterations were rapidly restored during arousal, maintaining the integrity of the ECM. Such an observation has never been reported in chronic lung diseases such as asthma and chronic obstructive pulmonary disease, where remodeling is an important hallmark, contributing to airway obstruction and hyper-reactivity (Barnes et al., 2002; Demedts et al., 2005). Several mechanisms may add to remodeling, including dysregulation of matrix metalloproteinase (MMP) activity and activation of the immune system, leading to influx of inflammatory cells into the airways (Greenlee et al., 2007; Redington, 2000), possibly in response to the excess generation of oxygen radicals during arousal (Okamoto et al., 2006). So far, the mechanisms governing the apparent 'physiological' remodeling of lung during hibernation, including its rapid reversibility, are unknown.

In this study we investigated processes driving lung remodeling in hibernation by examination of inflammatory markers and changes in ECM composition during torpor and arousal phases in the

hibernating hamster. We found only minor signs of immune activation, consistent with suppression of the immune function occurring in torpor (Bouma et al., 2011). We did observe substantial changes in ECM composition and the inhibition of MMP activity during torpor. As we recently found cooling to induce H_2S production through the endogenous enzyme cystathionine beta synthase (CBS) in hamster smooth muscle cells (Talaei et al., 2011a), and H_2S inhibits the abnormal accumulation of collagen in pulmonary arteries in hypoxic remodeling in rats (Zhang et al., 2005), we additionally investigated the involvement of H_2S. Because H_2S has been implicated in the inhibition of both inflammation (Zhang et al., 2008) and Zn^{2+}-dependent enzymes, such as MMPs (Laggner et al., 2007), we also studied the action of H_2S on lung sample gelatinase activity *in vitro*.

MATERIALS AND METHODS
Experimental procedures and hibernation model
Twenty (male and female) Syrian golden hamsters (*Mesocricetus auratus* Waterhouse 1839) were subjected to a hibernation protocol as previously described (Talaei et al., 2011b). In brief, hamsters were housed at ambient temperature (8 h:16 h light:dark) for at least 5 weeks. Subsequently, ambient temperature was lowered from 20 to 5°C and light conditions were changed to continuous dim red light (<1 lx). These conditions were maintained until the animals were killed. Movement of all animals was continuously monitored with passive infrared detectors. Periods with >24 h of inactivity were considered to be torpid phases. Animals were allowed to hibernate for several weeks in order to maximize torpor bout duration. Arousal occurred naturally without outside stimuli or changes in ambient temperature. Subsequently, animals were killed 24 h after torpor entrance (torpor early; *N*=4), >96 h after torpor entrance (torpor late; *N*=4), 2.5 h after the onset of arousal (early arousal; *N*=4) and 8.5 h after the onset of arousal (late arousal; *N*=4). Summer euthermic animals (*N*=4) served as controls, and were continuously housed at summer conditions (14 h:10 h light:dark; 21±1°C) and did not show torpor/arousal patterns. The experiments were approved by the Animal Experiments Committee of the University of Groningen (DEC#4746). Animals were killed by means of an intraperitoneal injection of 1.5 ml 6% sodium pentobarbital. Lungs from each phase were either flash-frozen in liquid nitrogen and kept at −80°C for molecular analysis or fixed for pathohistological analysis. For western blot and collagen content analyses, frozen lungs were homogenized (20% w/v) in ice-cold RIPA buffer [1% Igepal ca-630, 1% sodium dodecyl sulfate (SDS), 5 mg ml⁻¹ sodium deoxycholate, 1 mmol l⁻¹ sodium orthovanadate, 10 mmol l⁻¹ β-mercapto-ethanol, 40 μg ml⁻¹ phenylmethanesulfonyl fluoride (PMSF), 100 μg ml⁻¹ benzamidine, 500 ng ml⁻¹ pepstatin A, 500 ng ml⁻¹ leupeptine and 500 ng ml⁻¹ aprotinin in phosphate buffered saline (PBS)].

Antibodies and drugs
Antibodies against ICAM-1 (Santa Cruz SC-1511), VCAM-1 (Santa Cruz SC-1504, Santa Cruz Biotechnology, Santa Cruz, CA, USA), CBS (Santa Cruz SC-46830), NF-κB p65 (Santa Cruz SC-8008) and CD45 (Santa Cruz SC-25590) were used for western blot analysis and immunohistochemic stainings in tissue sections. Aminooxyacetic acid (AOAA; 10 mmol l⁻¹, Sigma C13408, Sigma-Aldrich, St Louis, MO, USA) was used as an inhibitor of CBS, and propargyl glycine (PG; 10 mmol l⁻¹, Sigma p7888) was used as an inhibitor of cysthationine gamma lyase (CSE) at a pH of 7.4.

Lung immunohistochemistry
For immunohistological evaluation, lungs were immersion-fixed in a zinc buffer containing 0.5% zinc chloride, 0.5% zinc acetate in 0.1 mol l⁻¹ Tris base buffer containing 0.05% calcium acetate, pH 7.4 (Wester et al., 2003), without inflation or flushing, which leads to preservation of the luminal content. To ensure proper penetration of the fixative, lungs were sliced midway and fixed for 24 h at room temperature. Subsequently, lungs were embedded in paraffin, cut into 3 μm sections, deparaffinized and submitted to staining for general examination of lung morphology (Hocher et al., 1999). Picrosirius Red staining was performed to visualize total hydroxyproline content of the lung. Antibody staining (ICAM-1, CBS, CD45) was performed by incubating sections with primary antibodies (1:100) with 1% bovine serum albumin (BSA) for 1 h followed by washing three times with PBS. Next, sections were incubated with secondary antibodies (1:100) with 1% BSA and 1% hamster serum for 1 h and subsequently washed three times with PBS. Dako AEC+High sensitivity substrate chromogen (K3461, Glostrup, Denmark) was used to visualize the antibody stain. Haematoxylin counterstaining was performed on all the samples to visualize the nuclei. To demonstrate the localization of each protein, images were captured using a Nikon 50i light microscope (Nikon, Amstelveen, The Netherlands) with a PAXcam camera (Midwest Information Systems, Villa Park, IL, USA). CD45-positive cells as indicators of leukocytes were counted in 10 fields per sample at 40× magnification and an average was calculated.

Real-time qPCR
In addition to immunostaining, the presence of leukocytes in lungs was analyzed by qPCR of CD45 (leukocyte common antigen), which is an essential regulator of T- and B-cell antigen receptor signaling (Zola et al., 1990). In brief, RNA was extracted from each sample using the Nucleospin tissue kit (catalog no. 740955.250, Macherey-Nagel, Düren, Germany). RNA (1 μg) was reverse transcribed in a reaction mixture (20 μl) containing 1 μl of random hexamers, 0.5 μl of RNase inhibitor, deoxynucleotide triphosphates (0.2 μl), 1 μl of reverse transcriptase, 4 μl RT buffer and Tris buffer (pH 7.4) at 37°C. Specific primers to CD45 (forward: AAGGCGACAGAGAG-ATGTCTGATGGTG, reverse: CTGTGTCCTCCAGCTCCTGT-ATGAA) and β-actin (forward: AAGATGACCC AGATCATG-TTTGAG and reverse: ACGTACATGGCTGGGGTGTTG) were synthesized (Base Clear, Leiden, The Netherlands). SYBR Green real-time PCR was performed using Bio-Rad CFX384 C1000 (Bio-Rad Laboratories, Hercules, CA, USA) and data were quantified with the Bio-Rad CFX manager 2.0 using reagents from the SYBR Green PCR-Master Mix (Qiagen, Hombrechtikon, Switzerland). The samples in the PCR 384-well plate were transferred to the thermal cycler and applied to the following protocol: predenaturation at 94°C (5 min; one cycle) followed by 35 cycles of denaturation at 94°C (30 s), annealing at 57°C (30 s), extension at 72°C (45 s) and a final extension at 72°C (8 min; one cycle), followed by a melting curve. All cycle threshold (C_t) values were collected at the exponential phase of the real-time qPCR. All data were normalized to β-actin.

Analysis of non-collagenous *versus* collagenous hydroxyproline
The lung content of total hydroxyproline, both collagenous and non-collagenous (e.g. hydroxyproline-rich glycoproteins), was measured spectrophotometrically (Junquiera et al., 1979). In brief, lungs were lysed on dry ice using RIPA buffer. Fifty micrograms of total lung lysates was mixed with 1 ml of Sirius Red reagent to measure total hydroxyproline content. To measure the collagenous part, collagen

was isolated from 50 μg of tissue lysates by 50 μl of $0.5 \, \text{mol} \, l^{-1}$ acetic acid at 4°C overnight. One milliliter of Sirius Red reagent was added to each extract. The samples were vortexed for 2 min and mixed for 30 min at room temperature. Subsequently, the samples were centrifuged for 5 min at 10,000 g and unbound dye was washed off with 1 ml of $0.1 \, \text{mol} \, l^{-1}$ HCl. One milliliter of $0.5 \, \text{mol} \, l^{-1}$ NaOH was added to each sample and the tubes were vortexed to release the bound dyes. The color intensity of Sirius Red was measured at 540 and 570 nm by a microplate reader (Jimenez et al., 1985). A collagen standard curve was used to measure the concentration of hydroxyproline in each sample. The amount of non-collagenous hydroxyproline was measured by subtracting the amount of collagenous hydroxyproline from the total amount of hydroxyproline (collagenous and non-collagenous), and the ratio of non-collagenous/collagenous hydroxyproline was calculated.

Determination of H$_2$S concentration
The Methylene Blue method for H$_2$S detection was applied to quantitatively measure the amount of free H$_2$S (Li et al., 2011; Qu et al., 2006) in lung samples obtained from hamsters in different phases of hibernation. Pieces of lungs were homogenized without thawing in ice-cold $50 \, \text{mmol} \, l^{-1}$ potassium phosphate buffer, pH 8.0 (12% w/v) on dry ice. The homogenate was centrifuged (47,000 g for 10 min at 4°C) and the supernatant (75 μl) was mixed with 0.25 ml Zn acetate (1%) and 0.45 ml water for 10 min at room temperature. Trichloroacetic acid (TCA; 10%, 0.25 ml) was then added to precipitate proteins followed by centrifugation (14,000 g for 10 min at 4°C). The clear supernatant obtained from lung homogenates was mixed with N,N-dimethyl-p-phenylenediamine sulfate ($20 \, \text{mmol} \, l^{-1}$; 133 μl) in $7.2 \, \text{mol} \, l^{-1}$ HCl and FeCl$_3$ ($30 \, \text{mmol} \, l^{-1}$; 133 μl) in $1.2 \, \text{mol} \, l^{-1}$ HCl. After 20 min, absorbance was measured at 670 nm. Blanks were made following the same procedure without samples. The concentration of H$_2$S was calculated by extrapolation using a standard curve obtained from different concentrations of Methylene Blue and spectrophotometric measurement at a wavelength of 670 nm.

MMP activity assay
A matrix protein assay was conducted according to Isaksen and Fagerhol (Isaksen and Fagerhol, 2001) with minor modifications. In brief, wells of a microplate (MaxiSorp; Nunc, Roskilde, Denmark) were coated with gelatin (Sigma-Aldrich), washed four times for 20 min with 300 μl distilled water, and stored overnight in distilled water at 4°C. The next day, the water was removed and wells were dried at 37°C for 30 min, covered with a plastic plate sealer (Microseal, Bio-Rad Laboratories) and stored at –20°C until use. To activate gelatinases in lysed lung samples each containing 100 μg of protein, 200 μl of TNC buffer ($50 \, \text{mmol} \, l^{-1}$ Tris, $150 \, \text{mmol} \, l^{-1}$ NaCl, $5 \, \text{mmol} \, l^{-1}$ CaCl$_2$, $10 \, \mu\text{mol} \, l^{-1}$ ZnCl$_2$, 0.01% BRIJ 35, pH 7.6) containing $0.2 \, \text{mmol} \, l^{-1}$ p-aminophenylmercuric acetate/ dimethylsulfoxide (APMA/DMSO) was added to each well (N=3). Wells were covered with a plastic plate sealer and incubated for 22 h at 37°C, washed three times for 10 min with distilled water and tapped dry. A Bradford assay was performed on the residual gelatin left at the bottom of the wells. To investigate whether the addition of NaHS inhibited MMP activity, $500 \, \mu\text{mol} \, l^{-1}$ of NaHS was added to the euthermic samples at room temperature and incubated for 2 h. To investigate the level of reconstitution of the enzyme after inhibition, Tris buffer containing extra zinc ion as ZnSO$_4$ ($500 \, \mu\text{mol} \, l^{-1}$) and NaCl ($75 \, \text{mmol} \, l^{-1}$) at pH 7.4 was added to NaHS-treated euthermic samples and the same procedure as above was followed for these samples after 5 h of incubation at room

temperature. Control wells containing only gelatin with no sample were used as reference. The absorption was read at 720 nm using a microplate reader.

Angiotensin-1 converting enzyme activity assay
Angiotensin-1 converting enzyme activity was determined using the procedure described by Conroy and Lai (Conroy and Lai, 1978) with some modifications. Hamster lungs were employed as the enzyme source. Concentrated proteins (50 μl) homogenized in $50 \, \text{mmol} \, l^{-1}$ potassium phosphate buffer pH 7.5 were incubated with 200 μl of substrate buffer ($0.5 \, \text{mol} \, l^{-1}$ K$_2$HPO$_4$, $1.5 \, \text{mol} \, l^{-1}$ NaCl pH 8.5) for 20 min at room temperature. Samples (50 μl) were incubated with 50 μl of the synthetic substrate Hippuryl-His-Leu at sub-saturating concentrations ($1 \, \text{mmol} \, l^{-1}$). The tubes were vortexed and left at 37°C for 1 h. The enzyme reaction was stopped by addition of 100 μl of $1 \, \text{mol} \, l^{-1}$ NaOH. Then, 50 μl of 1% o-phtaldehyde (OPA; Sigma H4884) in methanol was added to each tube. To investigate the activity of H$_2$S on this enzyme, NaHS ($500 \, \mu\text{mol} \, l^{-1}$) was added to euthermic samples. The samples were left at room temperature for 2 h and the above procedure was followed. To investigate the level of reconstitution of the enzyme after inhibition, Tris buffer containing zinc ion as ZnSO$_4$ ($500 \, \mu\text{mol} \, l^{-1}$) and NaCl ($75 \, \text{mmol} \, l^{-1}$) at pH 7.4 was added to NaHS-treated euthermic samples and the above procedure was followed for these samples after 5 h of incubation at room temperature. Fluorescence was immediately determined at 355/490 nm. Enzyme activity is expressed as nmol His-Leu formed mg^{-1} protein h^{-1}.

Western blot analysis
In lung lysates, the protein concentration was determined by the Bradford protein assay (Bradford, 1976). Western blotting was used to quantify the expression of ICAM-1, VCAM-1, NF-κB (P65) and CBS. For each sample, 20 μl of loading buffer (10% SDS, 50% glycerol, $0.33 \, \text{mol} \, l^{-1}$ Tris HCl pH 6.8, 0.05% Bromophenol Blue) was added to every 50 μg of protein and loaded onto pre-made gradient gels 4–20% (Thermoscientific, Waltham, MA, USA) for electrophoresis at 100 V (80 min). The gels were subsequently blotted on nitrocellulose membranes. Proteins on the nitrocellulose membranes were detected with specific primary antibodies (1:1000) overnight at 4°C, washed three times with TBS+Tween solution and treated with the related secondary antibody (1:1000, 2 h at room temperature). The membranes were developed using super signal West Dura substrate (Thermoscientific) and GeneSnap (version 6.07, Syngene, Cambridge, UK) was used to acquire images. The results were analyzed using GeneTools version 3.08 (Syngene).

Statistics
All data are presented as means ± s.d. Differences between the groups were compared using a one-way ANOVA (P<0.05) with a $post\ hoc$ Tukey's test (GraphPad Prism version 5.00 for Windows, GraphPad Software, La Jolla, CA, USA), unless indicated otherwise.

RESULTS
Inflammatory markers in lung tissue
To substantiate inflammatory processes involved in remodeling in lung of hibernating hamster, several molecular markers were investigated. Increased expression of ICAM-1 and VCAM-1 are implicated in the inflammatory response and lung remodeling. The expression of both ICAM-1 (Fig. 1A) and VCAM-1 (Fig. 1E) was modestly but significantly higher during torpor compared with euthermia or arousal, as measured by western blotting. ICAM-1
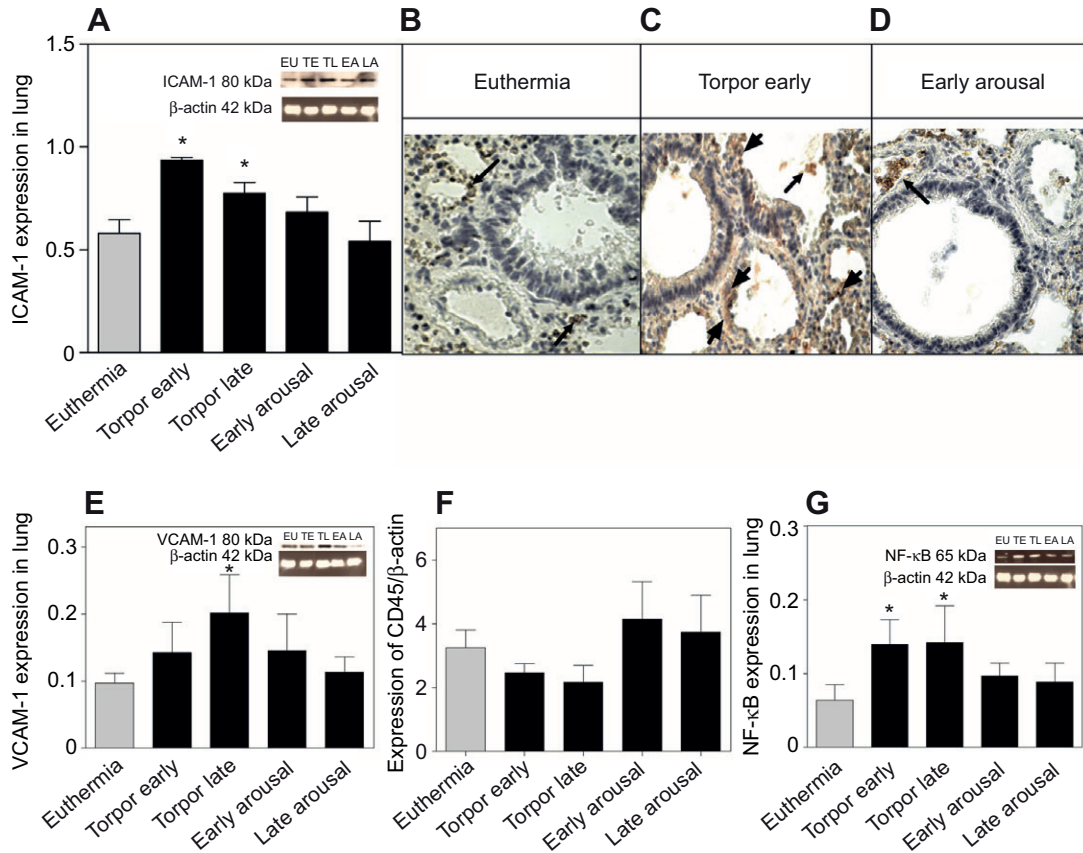
Fig. 1. Inflammatory response in hamster lungs during different phases of hibernation. (A) Expression of ICAM-1 in lung tissue of hibernating Syrian hamsters. The highest expression for ICAM-1 is observed during torpor early. (B–D) The expression of ICAM-1 in tissue slides (3 μm) is mainly located in the epithelial and endothelial cells of the vessels and alveoli (40× magnification). Thin arrows indicate erythrocytes and thick arrows indicate ICAM-1 stain with ACE chromogen. (E) VCAM-1 expression in lung tissue of hibernating hamster increases during torpor and normalizes during arousal. (F) PCR analysis of the expression of CD45 as a marker present on leukocytes relative to β-actin. (G) Western blot analysis of the expression of NF-κB P65 (the major subunit of nuclear factor B) as a marker of an inflammatory response. NF-κB increases during torpor and returns to normal levels during arousal. Protein expression is normalized to β-actin expression. Data are means ± s.d. ($N \geq 3$ per group); *, significantly different from euthermia, $P < 0.05$. EU, euthermia; TE, torpor entrance; TL, torpor late; EA, early arousal; LA, late arousal.

immunohistochemical staining demonstrated a higher expression in different compartments such as vessels, airways and the alveoli during torpor (Fig. 1B–D).

The number of CD45-positive cells as the main marker of leukocytes was examined histologically and did not differ between groups, the average of 10 microscopic fields per animal (40×) was 1.5±0.3, 1.4±0.2 and 1.6±0.2 cells in early torpor, early arousal and euthermia, respectively. Given the low number of leukocytes, we aimed to further substantiate changes in the number of cells by investigating the presence of CD45 in lung tissue by PCR. No significant changes in CD45 expression were found in tissue during torpor compared with euthermia or arousal (Fig. 1F).

Finally, expression of p65, the major subunit of NF-κB was measured. Its expression was increased during torpor phases, and decreased in arousal to euthermic levels (Fig. 1G).

Together, these results indicate a modest increase in some of the markers of inflammation in lungs during the torpor phase.

Matrix protein analysis and MMP activity

In our previous study, we found that the expression of collagenous hydroxyproline increased in the lung during early torpor, followed by normalization to euthermic values during late torpor and arousal (Talaei et al., 2011b). In line with our previous findings,

hydroxyproline staining was intensified in lung samples obtained during the torpor phase compared with euthermia or arousal (Fig. 2A–D). Also, non-collagenous hydroxyproline expression increased during torpor, reaching a fourfold increase in late torpor compared with euthermia (Fig. 2E). Subsequently, non-collagenous hydroxyproline decreases in early arousal and returns to normal levels at late arousal. As a consequence, the ratio of non-collagenous hydroxyproline to collagenous hydroxyproline was particularly increased during late torpor and normalized in late arousal (Fig. 2F).

Because of large changes in hydroxyproline content between torpor and arousal phases, MMP2 and MMP9 activity in lung lysates was assessed. Gelatinase activity was significantly suppressed during torpid phases and to a lesser extent in late arousal (Fig. 2F).

CBS expression and H₂S measurements

We previously found that cooling induced production of H₂S in Syrian hamster cells (Talaei et al., 2011a). As H₂S inhibits ACE, a Zn²⁺-dependent enzyme (Laggner et al., 2007) implicated in lung remodeling (Kuba et al., 2006), we measured the H₂S content of lung tissue. H₂S content doubled in torpor and early arousal and normalized to euthermic levels in late arousal (Fig. 3F). Because of
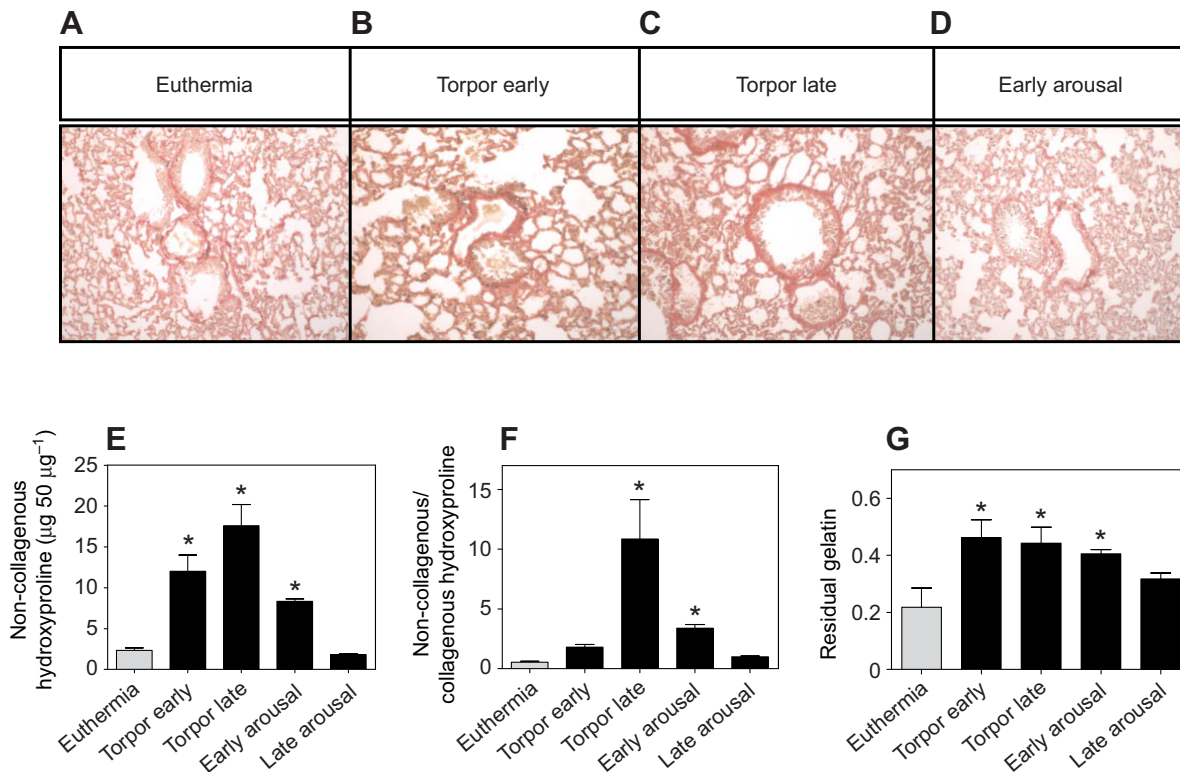
Fig. 2. Changes in non-collagenous *versus* collagenous hydroxyproline measured by Sirius Red staining in lung tissue of hibernating hamsters. (A–D) Hydroxyproline expression in lung tissue samples obtained from different phases of hibernation (20× magnification). (E) Non-collagenous hydroxyproline expression is increased during torpor and early arousal. (F) The expression ratio of non-collagenous/collagenous hydroxyproline increases, in particular during torpor late. (G) Spectrophotometric measurement of gelatin degradation/gelatinase assay shows a low activity of gelatinases in lungs obtained from animals in torpor and early arousal. High measures signify lower gelatinase activity. Data are means ± s.d. (N≥3 per group); *, significantly different from euthermia, $P<0.05$.

increased H_2S content, we examined expression of CBS, one of the main enzymes involved in H_2S production *in vivo*. Western blot analysis of lung tissue demonstrated a doubling of CBS expression during early and late torpor and a rapid normalization during arousal to euthermic levels (Fig. 3E). Further, immunohistochemistry demonstrated an increase in CBS expression in lung from torpid hamsters, mainly in the endothelial cells of the alveoli and bronchi (Fig. 3A–D).

H_2S modulates MMP and ACE activity *in vitro*

To substantiate the potential of H_2S to suppress MMP activity *via* quenching of Zn^{2+}, gelatinase activity was assessed *in vitro* in the presence of excess Zn^{2+}, with NaHS as an H_2S donor, and AOAA, an inhibitor of CBS. Administration of NaHS ($500\,\mu mol\,l^{-1}$) to protein obtained from euthermic samples significantly decreased gelatinase activity, which was attenuated by adding excess Zn^{2+} (Fig. 4A). In contrast, inhibition of CBS with AOAA significantly increased gelatinase activity in all groups (Fig. 4A). The inhibition of cystathionine gamma lyse (CSE) by propargyl glycine did not affect gelatinase activity in all groups (data not shown).

To verify our findings on another Zn^{2+}-dependent enzyme, the influence of AOAA on lung ACE activity was measured. Inhibition of AOAA substantially increased ACE activity in lung proteins of torpid animals and slightly in euthermic animals (Fig. 4B). However, AOAA did not affect ACE activity in aroused animals. In contrast, the ACE inhibitor captopril inhibited ACE

activity in all animal groups, but also to a lesser extent in arousal groups (Fig. 4B).

DISCUSSION
The goal of the present study was to obtain insight into the mechanisms causing substantial, but reversible, lung remodeling during the torpor phase of hibernation in the Syrian hamster, as described previously (Talaei et al., 2011b). The three major observations of this study were as follows. First, remodeling coincided with decreased MMP-2/MMP-9 and ACE activity. Second, remodeling coincided with increased levels of H_2S, explained by an increase in CBS expression. Finally, only a modest activation of inflammatory markers was observed, which was restricted to the torpor phase. These results indicate that an increased production of H_2S through CBS in hamster lungs during torpor contributes to remodeling by inhibition of gelatinase activity and possibly by suppression of the inflammatory response (for a diagram, see Fig. 5). Moreover, this is the first report implicating a functional role of endogenous H_2S production in natural hibernation. In the present study, we focused on biochemical changes of the lung during remodeling rather than histopathological analysis. The latter is hampered by the fact that lungs were not inflated when the animals were killed. Thus, analysis of the histological changes in torpor and their rapid reversibility during arousal in the lungs of these hamsters is restricted to large airways and has been described previously (Talaei et al., 2011b).
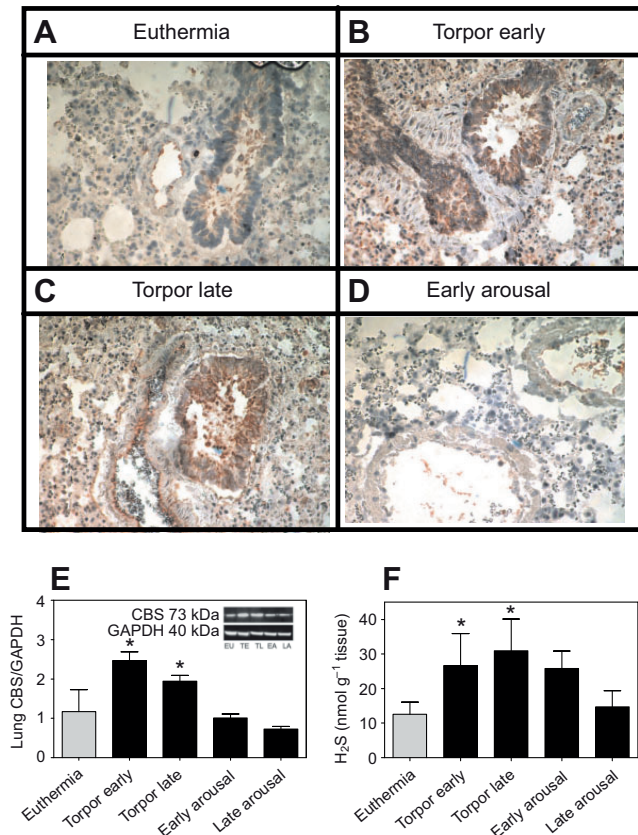
Fig. 3. Cystathionine beta synthase (CBS) expression and H₂S concentration increase during torpor in lung tissue from hibernating hamsters. (A–D) Expression of CBS in lung tissue slides (3 μm) of hibernating hamsters. The expression is mainly located in the epithelial and endothelial cells of the vessels and alveoli (40× magnification). (E) Expression of CBS in lungs is increased during torpor and early arousal. CBS expression is normalized to GAPDH. (F) Lung H₂S concentration rises during torpor and early arousal and returns to normal levels in late arousal. Data are means ± s.d. (*N*≥3 per group); *, significant difference from euthermia (gray bars), *P*<0.05.

Lung remodeling, as previous reported, consisted of a substantial increase in lung collagen, determined by Picrosirius Red staining. It is known that Sirius Red binds to hydroxyproline present in all major constituents of ECM, including collagens, proteoglycans and adhesive glycoproteins (Uitto and Larjava, 1991). In the present study, we observed that the increased intensity of staining during the torpor phase was accompanied by a substantial increase in the ratio of non-collagenous to collagenous hydroxyproline, particularly in late torpor. Most likely, the increase in the amount of non-collagenous hydroxyproline reflects unwinding and the break-down of the extracellular matrix by MMP activity (Chung et al., 2004), which is probably mainly due to activity of the gelatinases MMP-2 and MMP-9 (Corbel et al., 2000). Therefore, the changes in MMP activity may well underlie the lung remodeling as observed in hibernation, and these changes are probably related to low temperatures. Indeed, previous analyses of striated muscle, brain and circulating immune cells represent cases in which changes are specific to hibernation or driven by lowered body temperature (Bouma et al., 2011; Nowell et al., 2011; von der Ohe et al., 2006).

Recent publications suggest an involvement of H₂S in lung remodeling. For instance, endogenous H₂S prevented pulmonary collagen remodeling induced by high pulmonary blood flow (Li et

al., 2009). In addition, downregulation of the endogenous H₂S pathway in lungs was shown to induce structural remodeling of pulmonary vasculature (Xiaohui et al., 2005). Likewise, the release of H₂S from NaHS inhibits the proliferation of pulmonary artery smooth muscle cells and reduces the expression of collagen in pulmonary arteries of rats under hypoxia (Hongfang et al., 2006).

Our study implies that H₂S production regulates MMP activity during hibernation by quenching Zn²⁺. Direct evidence is derived from the experiments where excess Zn²⁺ overcomes the inhibition of gelatinase activity, whereas NaHS shows the opposite. We found that an increased level of H₂S in lungs during torpor coincided with upregulation of CBS. The increase in gelatinase activity following addition of AOAA to samples suggests that there is a direct link between MMP activity and H₂S production. These results are in accord with our observation that H₂S inhibits ACE through a previously identified interation between H₂S and Zn²⁺ (Laggner et al., 2007). Interestingly, decreased tissue and plasma ACE activity was shown in the hibernating 13-lined ground squirrel (Weekley, 1995). Thus, we propose that an increased H₂S production in torpor inhibits gelatinase and ACE activity because of the quenching of Zn²⁺. This study is the first to implicate the H₂S route as an adaptive molecular mechanism in natural hibernation.

Because of the involvement of the immune system in lung remodeling, inflammatory markers in lungs from hamsters were studied. We found no significant change in the CD45 expression in lungs throughout the hibernating phases. Thus, it is reasonable to assume that extravasation of leukocytes into the lung tissue is absent during arousal, notwithstanding the presence of normal numbers of circulating leukocytes (Bouma et al., 2011). In accord, expression of NF-κB (P65), ICAM-1 and VCAM-1 normalized to euthermic levels during arousal, which may prevent excess adhesion and infiltration of immune cells into the tissue in arousal. Activation of NF-κB and production of NF-κB-dependent chemokines are thought to be involved in the pathogenesis of neutrophilic lung inflammation (Lancaster et al., 2001). In addition, upregulation of NF-κB (P65) in lungs is accepted as an indicator of the activation of immune cells and subsequent inflammatory mediator production (Di Stefano et al., 2002). Interestingly, it has been shown that the redox-sensitive transcription factor NF-κB is strongly activated in torpor phases in squirrel intestine (Carey et al., 2000). Furthermore, mice deficient in ICAM-1 are protected from airway inflammation, as assessed by accumulation of immune cells in airway tissue following an infection (Walter et al., 2002). Thus, our data do not support a substantial role of inflammatory processes in lung remodeling during hibernation. Instead, our data suggest that lung remodeling is dependent on the H₂S-dependent rapid regulation of MMP activity. Indeed, it is already known that during hibernation, arousal represents a period of intense proteolysis for gluconeogenesis, which diminishes the content of proteins in tissues (Lechner, 1985; Lohuis et al., 2005).

Recently, H₂S has been implicated in the alleviation of organ damage by decreasing the synthesis of pro-inflammatory cytokines, reducing leukocyte adherence and diapedesis, and protecting organs from oxidative injury (Esechie et al., 2008). In a study on lung injury induced by burn and smoke inhalation in a murine model, a parenteral formulation of H₂S reduced interleukin (IL)-1β levels and increased the anti-inflammatory cytokine IL-10, thereby reducing lung injury (Esechie et al., 2008). H₂S-releasing non-steroidal anti-inflammatory drugs constitute a potential treatment for pancreatitis-associated acute lung injury/acute respiratory distress syndrome (Bhatia et al., 2008). It has been proposed that the H₂S-releasing properties of such formulations inhibit the DNA binding activity of
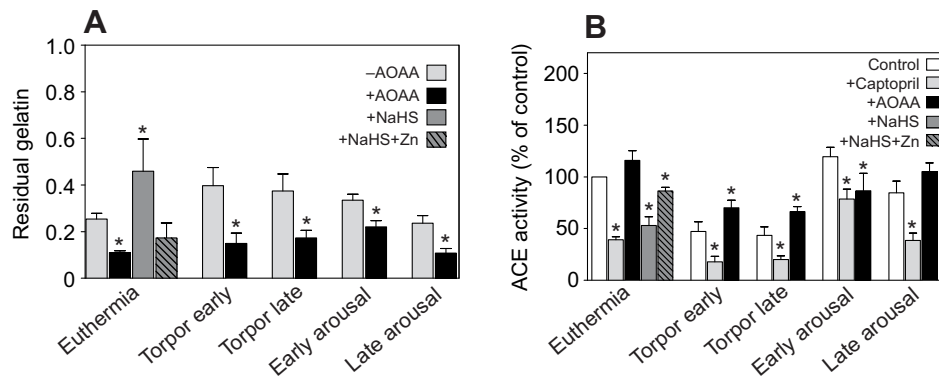
Fig. 4. Inhibitory action of H$_2$S on gelatinase and angiotensin converting enzyme (ACE) activity. (A) Results from the gelatin degradation assay show a decreased activity of gelatinases in lungs obtained from animals in torpor and early arousal. Inhibition of CBS by aminooxyacetic acid (AOAA; 10 mmol l^{-1}) normalizes gelatinase degradation to control levels. Addition of NaHS (500 µmol l^{-1}) inhibits gelatinase degradation, which is overcome by the addition of extra zinc ion as ZnSO$_4$ (500 µmol l^{-1}). Higher residual gelatin signifies lower gelatinase activity in samples. (B) ACE activity in lungs of euthermic or hibernating Syrian hamsters in the presence or absence of captopril, as an ACE inhibitor, or AOAA, as an inhibitor of CBS/H$_2$S formation. Decreased ACE activity during torpid phases was increased by addition of AOAA. NaHS reduced ACE activity, which was reversed by addition of extra Zn^{2+}. ACE activity is expressed as percent of ACE activity in euthermic hamsters. Data are means ± s.d. ($N \geq 3$ per group); *, significant difference to control, $P<0.05$.

nuclear transcriptional factors (AP-1 and NF-κB) and subsequent production of inflammation-related genes (Li et al., 2007). Additionally, H$_2$S administration attenuates protein oxidation following injury and improves the histological condition of the lung. Thus, H$_2$S has been proposed to protect lungs through anti-inflammatory and antioxidant pathways (Esechie et al., 2008). However, controversial observations with respect to the beneficial effects of H$_2$S have also been reported. For example, administration of NaHS to normal mice causes a significant increase in DNA binding activity of NF-κB and production of adhesion molecules (Zhang et al., 2007a; Zhang et al., 2007b). The different animal models and different doses of H$_2$S donors used might be the main reason for the inconsistency observed in regulation of leukocyte activity and inflammatory response by H$_2$S. It is possible that the modulation of the endogenous H$_2$S production, particularly through the H$_2$S-producing enzyme CBS, is superior to exogenous administration of H$_2$S donors.

Further, it remains elusive whether lung remodeling during hibernation is precipitated by factor(s) that are specific to hibernation, or is merely a consequence of the low temperature of lung tissue during torpor or changes in airway temperature because of the inhalation of large quantities of cold air during the hypermetabolic stages of pre-torpor and early arousal when animals are hyperventilating. Previous analyses of striated muscle, brain and circulating immune cells represent cases in which changes are specific to hibernation or driven by lowered body temperature (Bouma et al., 2011; Nowell et al., 2011; von der Ohe et al., 2006).

To date, the physiological significance of lung remodeling during hibernation remains unclear, as does the factor that triggers it. We previously speculated that the remodeling response may protect airways against collapse during torpor (Talaei et al., 2011b) when mean breathing frequency is reduced to a few breaths per minute and apneic periods of considerable length exist (Elvert and Heldmaier, 2005). When extended into the arousal phase, airway collapse would preclude the necessary adaptive hyperventilation and jeopardize the animal's survival.

Our finding that H$_2$S production is modulated during hibernation, and is increased during torpor in particular, may have implications beyond organ remodeling, i.e. for the process of natural hibernation itself. H$_2$S inhalation is known to induce metabolic suppression in non-hibernating mammals, inducing a hibernation-like state referred to as 'suspended animation' (Van Raemdonck, 2010). Increased endogenous H$_2$S formation may contribute to the lowering of metabolism during this phase of hibernation. Also, H$_2$S has recently emerged as a novel gasotransmitter with a cellular protective action *in vitro* and *in vivo* on brain, lungs and the cardiovascular system (for reviews, see Ji et al., 2008; Körtner and Geiser, 2000). Increased H$_2$S levels during the early arousal phase may thus protect various organs of hibernators by providing additional antioxidant defense and suppressing apoptosis.
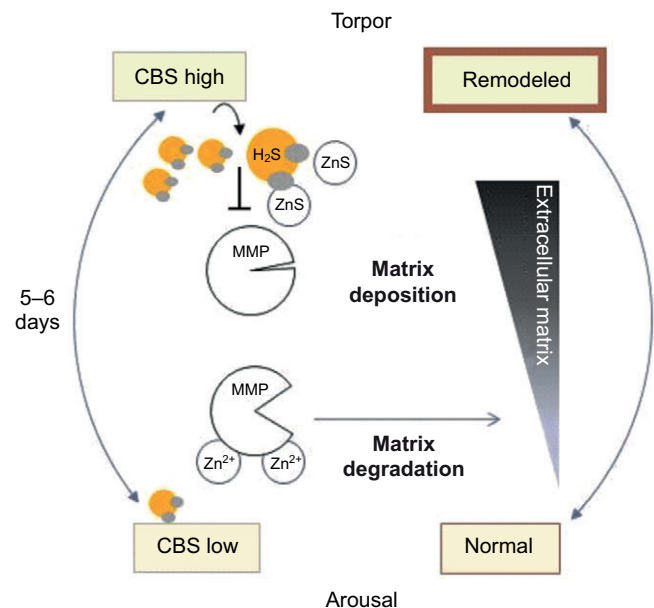

Fig. 5. Diagram illustrating the proposed effect of H$_2$S on lung remodeling during hibernation. Matrix metalloproteinase (MMP) activity is regulated by zinc (Zn^{2+}). In torpor, the increased CBS expression increases the production of H$_2$S and capturing of Zn^{2+}, in turn inhibiting MMP activity and thus promoting a deposition of extracellular matrix. In arousal, CBS expression and H$_2$S levels are low. As a consequence, MMPs are able to degrade the extracellular matrix.

In summary, in this study we identified increased production of H_2S through CBS in lungs of Syrian hamster during the torpor phase of hibernation, which inhibited gelatinase and ACE activity, thus contributing to the observed lung remodeling and possibly suppressing the inflammatory response.

REFERENCES

Arai, S., Hanaya, T., Sakurai, T., Ikeda, M. and Kurimoto, M. (2005). A novel phenomenon predicting the entry into a state of hibernation in Syrian hamsters (*Mesocricetus auratus*). *J. Vet. Med. Sci.* **67**, 215-217.

Barnes, P. J. and Thomson, N. C. Rennard and S. I. and Drazen J. M. (2002). *Asthma and COPD: Basic Mechanisms and Clinical Management.* San Diego, CA: Elsevier Science.

Bhatia, M., Sidhapuriwala, J. N., Sparatore, A. and Moore, P. K. (2008). Treatment with H2S-releasing diclofenac protects mice against acute pancreatitis-associated lung injury. *Shock* **29**, 84-88.

Bouma, H. R., Kroese, F. G. M., Kok, J. W., Talaei, F., Boerema, A. S., Herwig, A., Draghiciu, O., van Buiten, A., Epema, A. H., van Dam, A. et al. (2011). Low body temperature governs the decline of circulating lymphocytes during hibernation through sphingosine-1-phosphate. *Proc. Natl. Acad. Sci. USA* **108**, 2052-2057.

Bradford, M. M. (1976). A rapid and sensitive method for the quantitation of microgram quantities of protein utilizing the principle of protein-dye binding. *Anal. Biochem.* **72**, 248-254.

Carey, H. V., Frank, C. L. and Seifert, J. P. (2000). Hibernation induces oxidative stress and activation of NK-kappaB in ground squirrel intestine. *J. Comp. Physiol. B* **170**, 551-559.

Carey, H. V., Andrews, M. T. and Martin, S. L. (2003). Mammalian hibernation: cellular and molecular responses to depressed metabolism and low temperature. *Physiol. Rev.* **83**, 1153-1181.

Chung, L., Dinakarpandian, D., Yoshida, N., Lauer-Fields, J. L., Fields, G. B., Visse, R. and Nagase, H. (2004). Collagenase unwinds triple-helical collagen prior to peptide bond hydrolysis. *EMBO J.* **23**, 3020-3030.

Conroy, J. M. and Lai, C. Y. (1978). A rapid and sensitive fluorescence assay for angiotensin-converting enzyme. *Anal. Biochem.* **87**, 556-561.

Corbel, M., Boichot, E. and Lagente, V. (2000). Role of gelatinases MMP-2 and MMP-9 in tissue remodeling following acute lung injury. *Braz. J. Med. Biol. Res.* **33**, 749-754.

Demedts, I. K., Brusselle, G. G., Bracke, K. R., Vermaelen, K. Y. and Pauwels, R. A. (2005). Matrix metalloproteinases in asthma and COPD. *Curr. Opin. Pharmacol.* **5**, 257-263.

Di Stefano, A., Caramori, G., Oates, T., Capelli, A., Lusuardi, M., Gnemmi, I., Ioli, F., Chung, K. F., Donner, C. F., Barnes, P. J. et al. (2002). Increased expression of nuclear factor-kappaB in bronchial biopsies from smokers and patients with COPD. *Eur. Respir. J.* **20**, 556-563.

Elvert, R. and Heldmaier, G. (2005). Cardiorespiratory and metabolic reactions during entrance into torpor in dormice, *Glis glis*. *J. Exp. Biol.* **208**, 1373-1383.

Esechie, A., Kiss, L., Olah, G., Horváth, E. M., Hawkins, H., Szabo, C. and Traber, D. L. (2008). Protective effect of hydrogen sulfide in a murine model of acute lung injury induced by combined burn and smoke inhalation. *Clin. Sci.* **115**, 91-97.

Greenlee, K. J., Werb, Z. and Kheradmand, F. (2007). Matrix metalloproteinases in lung: multiple, multifarious, and multifaceted. *Physiol. Rev.* **87**, 69-98.

Hocher, B., George, I., Rebstock, J., Bauch, A., Schwarz, A., Neumayer, H. H. and Bauer, C. (1999). Endothelin system-dependent cardiac remodeling in renovascular hypertension. *Hypertension* **33**, 816-822.

Hongfang, J., Cong, B., Zhao, B., Zhang, C., Liu, X., Zhou, W., Shi, Y., Tang, C. and Junbao, D. (2006). Effects of hydrogen sulfide on hypoxic pulmonary vascular structural remodeling. *Life Sci.* **78**, 1299-1309.

Isaksen, B. and Fagerhol, M. K. (2001). Calprotectin inhibits matrix metalloproteinases by sequestration of zinc. *J. Clin. Pathol. Mol. Pathol.* **54**, 289-292.

Ji, Y., Pang, Q. F., Xu, G., Wang, L., Wang, J. K. and Zeng, Y. M. (2008). Exogenous hydrogen sulfide postconditioning protects isolated rat hearts against ischemia-reperfusion injury. *Eur. J. Pharmacol.* **587**, 1-7.

Jimenez, W., Parés, A., Caballería, J., Heredia, D., Bruguera, M., Torres, M., Rojkind, M. and Rodés, J. (1985). Measurement of fibrosis in needle liver biopsies: evaluation of a colorimetric method. *Hepatology* **5**, 815-818.

Junqueira, L. C. U., Bignolas, G. and Brentani, R. R. (1979). A simple and sensitive method for the quantitative estimation of collagen. *Anal. Biochem.* **94**, 96-99.

Körtner, G. and Geiser, F. (2000). The temporal organization of daily torpor and hibernation: circadian and circannual rhythms. *Chronobiol. Int.* **17**, 103-128.

Kuba, K., Imai, Y. and Penninger, J. M. (2006). Angiotensin-converting enzyme 2 in lung diseases. *Curr. Opin. Pharmacol.* **6**, 271-276.

Laggner, H., Hermann, M., Esterbauer, H., Muellner, M. K., Exner, M., Gmeiner, B. M. and Kapiotis, S. (2007). The novel gaseous vasorelaxant hydrogen sulfide inhibits angiotensin-converting enzyme activity of endothelial cells. *J. Hypertens.* **25**, 2100-2104.

Lancaster, L. H., Christman, J. W., Blackwell, T. R., Koay, M. A. and Blackwell, T. S. (2001). Suppression of lung inflammation in rats by prevention of NF-κB activation in the liver. *Inflammation* **25**, 25-31.

Lechner, A. J. (1985). Pulmonary design in a microchiropteran bat (*Pipistrellus subflavus*) during hibernation. *Respir. Physiol.* **59**, 301-312.

Li, L., Rossoni, G., Sparatore, A., Lee, L. C., Del Soldato, P. and Moore, P. K. (2007). Anti-inflammatory and gastrointestinal effects of a novel diclofenac derivative. *Free Radic. Biol. Med.* **42**, 706-719.

Li, X., Jin, H., Bin, G., Wang, L., Tang, C. and Du, J. (2009). Endogenous hydrogen sulfide regulates pulmonary artery collagen remodeling in rats with high pulmonary blood flow. *Exp. Biol. Med.* **234**, 504-512.

Li, Z., Wang, Y., Xie, Y., Yang, Z. and Zhang, T. (2011). Protective effects of exogenous hydrogen sulfide on neurons of hippocampus in a rat model of brain ischemia. *Neurochem. Res.* **36**, 1840-1849.

Lohuis, T. D., Beck, T. D. I. and Harlow, H. J. (2005). Hibernating black bears have blood chemistry and plasma amino acid profiles that are indicative of long-term adaptive fasting. *Can. J. Zool.* **83**, 1257-1263.

Morin, P., Jr and Storey, K. B. (2009). Mammalian hibernation: differential gene expression and novel application of epigenetic controls. *Int. J. Dev. Biol.* **53**, 433-442.

Nowell, M. M., Choi, H. and Rourke, B. C. (2011). Muscle plasticity in hibernating ground squirrels (*Spermophilus lateralis*) is induced by seasonal, but not low-temperature, mechanisms. *J. Comp. Physiol. B* **181**, 147-164.

Okamoto, I., Kayano, T., Hanaya, T., Arai, S., Ikeda, M. and Kurimoto, M. (2006). Up-regulation of an extracellular superoxide dismutase-like activity in hibernating hamsters subjected to oxidative stress in mid- to late arousal from torpor. *Comp. Biochem. Physiol.* **144C**, 47-56.

Qu, K., Chen, C. P., Halliwell, B., Moore, P. K. and Wong, P. T. (2006). Hydrogen sulfide is a mediator of cerebral ischemic damage. *Stroke* **37**, 889-893.

Redington, A. E. (2000). Fibrosis and airway remodeling. *Clin. Exp. Allergy* **30**, 42-45.

Talaei, F., Bouma, H. R., Van der Graaf, A. C., Strijkstra, A. M., Schmidt, M. and Henning, R. H. (2011a). Serotonin and dopamine protect from hypothermia/rewarming damage through the CBS/H2S pathway. *PLoS ONE* **6**, e22568.

Talaei, F., Hylkema, M. N., Bouma, H. R., Boerema, A. S., Strijkstra, A. M., Henning, R. H. and Schmidt, M. (2011b). Reversible remodeling of lung tissue during hibernation in the Syrian hamster. *J. Exp. Biol.* **214**, 1276-1282.

Uitto, V. J. and Larjava, H. (1991). Extracellular matrix molecules and their receptors: an overview with special emphasis on periodontal tissues. *Crit. Rev. Oral Biol. Med.* **2**, 323-354.

Van Raemdonck, D. (2010). Thoracic organs: current preservation technology and future prospects; part 1: lung. *Curr. Opin. Organ Transplant.* **15**, 150-155.

von der Ohe, C. G., Darian-Smith, C., Garner, C. C. and Heller, H. C. (2006). Ubiquitous and temperature-dependent neural plasticity in hibernators. *J. Neurosci.* **26**, 10590-10598.

Walter, M. J., Morton, J. D., Kajiwara, N., Agapov, E. and Holtzman, M. J. (2002). Viral induction of a chronic asthma phenotype and genetic segregation from the acute response. *J. Clin. Invest.* **110**, 165-175.

Weekley, L. B. (1995). Tissue and plasma peptidase activity is altered during hypothermic hibernation in the 13 lined ground squirrel (*Spermophilus tridecemlineatus*). *Physiol. Behav.* **57**, 595-598.

Wester, K., Asplund, A., Bäckvall, H., Micke, P., Derveniece, A., Hartmane, I., Malmström, P. U. and Pontén, F. (2003). Zinc-based fixative improves preservation of genomic DNA and proteins in histoprocessing of human tissues. *Lab. Invest.* **83**, 889-899.

Xiaohui, L., Junbao, D., Lin, S., Jian, L., Xiuying, T., Jianguang, Q., Bing, W., Hongfang, J. and Chaoshu, T. (2005). Down-regulation of endogenous hydrogen sulfide pathway in pulmonary hypertension and pulmonary vascular structural remodeling induced by high pulmonary blood flow in rats. *Circ. J.* **69**, 1418-1424.

Zancanaro, C., Malatesta, M., Mannello, F., Vogel, P. and Fakan, S. (1999). The kidney during hibernation and arousal from hibernation. A natural model of organ preservation during cold ischaemia and reperfusion. *Nephrol. Dial. Transplant.* **14**, 1982-1990.

Zhang, C. Y., Du, J. B., Yan, H. and Tang, C. S. (2005). Effect of a new gasotransmitter, hydrogen sulfide, on collagen remodeling of pulmonary artery under hypoxia. *Zhonghua Jie He He Hu Xi Za Zhi* **28**, 448-452.

Zhang, H., Zhi, L., Moochhala, S., Moore, P. K. and Bhatia, M. (2007a). Hydrogen sulfide acts as an inflammatory mediator in cecal ligation and puncture-induced sepsis in mice by upregulating the production of cytokines and chemokines via NF-kappaB. *Am. J. Physiol.* **292**, L960-L971.

Zhang, H., Zhi, L., Moochhala, S. M., Moore, P. K. and Bhatia, M. (2007b). Endogenous hydrogen sulfide regulates leukocyte trafficking in cecal ligation and puncture-induced sepsis. *J. Leukoc. Biol.* **82**, 894-905.

Zhang, H., Moochhala, S. M. and Bhatia, M. (2008). Endogenous hydrogen sulfide regulates inflammatory response by activating the ERK pathway in polymicrobial sepsis. *J. Immunol.* **181**, 4320-4331.

Zola, H., Melo, J. V., Zowtyj, H. N., Nikoloutsopoulos, A. and Skinner, J. (1990). The leukocyte-common antigen (CD45) complex and B-lymphocyte activation. *Hum. Immunol.* **27**, 368-377.